European Journal of Medicinal Chemistry 44 (2009) 3266–3271

Contents lists available at ScienceDirect

European Journal of Medicinal Chemistry

journal homepage: http://www.elsevier.com/locate/ejmech

Original article

A new type of five-membered heterocyclic inhibitors of basic metallocarboxypeptidases

Daniel Fernández, Francesc X. Avilés, Josep Vendrell*

Departament de Bioquímica i Biologia Molecular, Facultat de Biociències and Institut de Biotecnologia i de Biomedicina, Universitat Autònoma de Barcelona, E-08193 Bellaterra, Spain

ARTICLE INFO

Article history:
Received 29 December 2008
Received in revised form
20 February 2009
Accepted 26 March 2009
Available online 5 April 2009

Keywords:
Metallocarboxypeptidase
Protease M14 family
Human carboxypeptidase B
High-throughput screening
Molecular docking
1,3,4-Oxadiazole

ABSTRACT

A structure-based virtual screening survey was used to identify potential inhibitors of the human M14 family of metallocarboxypeptidases. A good correlation between docking energy scores and measured K_i values was observed, indicating an efficient performance of the screening procedure. Among various compounds displaying K_i values in the low micromolar range, *N*-(3-chlorophenyl)-4-((5-(3-methoxybenzylthio)-1,3,4-oxadiazol-2-yl)methyl)thiazol-2-amine emerged as the most powerful inhibitor for human carboxypeptidase B (CPB). According to molecular docking, this compound fits into CPB active site cleft through coordination of the catalytic zinc ion with the 1,3,4-oxadiazole moiety. This represents a novel five-membered heterocyclic type of inhibitor for disease-linked metallocarboxypeptidases and an interesting lead for further development.

1. Introduction

The M14 family of proteases (metallocarboxypeptidases, CPs) constitutes a widely distributed group of enzymes that perform different physiological functions [1]. This large family of metallocarboxypeptidases contains two subfamilies represented by the prototypical CPA and CPB forms and has been expanded by the recent discovery of a completely new subfamily [2]. Different CPs may participate in normal tissue organogenesis [3,4] as well as in pathological processes like pancreatic diseases [5], inflammation [6], fibrinolysis [7] and cancer [8,9]. Pharmaceutically relevant M14 members include human CPA2, mast cell carboxypeptidase (CPA3), and plasma CPB (also known as CPB2, CPR, CPU or TAFI) [10–12]. The development of novel diagnostic or chemotherapeutic tools may warrant a better understanding of M14 protease activities [13,14]. Several groups reported on the discovery of small-molecule inhibitors targeted to CPs [15,16]. One of these molecules, a peptidomimetic TAFI inhibitor, (*S*)-2-[3-(aminomethyl)phenyl]-3-{hydroxyl[(*R*)-2-methyl-1-{[(3-phenylpropyl)sulfonyl] amino propyl] phosphoryl propanoic acid showed promising properties when tested in animal models of thrombotic disease [17,18]. However, despite much effort that has been cast in the development of chemotherapeutic agents targeted to M14 proteases, a clinically useful molecule awaits to be discovered.

The work discussed here was aimed to the discovery of novel small-molecule organic ligands that might be useful leads for M14 protease drug design [19]. We employed a structure-based virtual screening methodology to query a diverse, non-focused, non-prefiltered, small-molecule database using the 3D crystal structure of human CPB as the template. This high-throughput screening survey afforded a number of hits out of which 25 were purchased and their K_i values measured in vitro. Although the correlation between the measured K_i values and the docking energy score is good for most compounds, a few exceptions suggest some drawbacks in the selection process. A five-membered heterocyclic compound with low micromolar CPB inhibitory potency emerged from the kinetic activity measurements. Molecular docking of such inhibitor indicated that binding to the catalytic zinc ion is mediated by its 1,3,4-oxadiazole moiety, a feature that distinguishes it from other known inhibitors. Thus, we report here on the discovery of a new type of metallocarboxypeptidase inhibitor scaffold and discuss on its potential for further developments.

2. Results and discussion

2.1. Bioinformatics: screening of small-molecule compounds

The molecules indicated in Fig. 1 are those which were available for purchase from the final set of compounds retrieved after careful automatic and manual filtering. The manual filtering took into

* Corresponding author. Tel.: +34 93 581 2375; fax: +34 93 581 1264.
E-mail address: josep.vendrell@uab.cat (J. Vendrell).

0223-5234/$ – see front matter © 2009 Elsevier Masson SAS. All rights reserved.
doi:10.1016/j.ejmech.2009.03.034

1

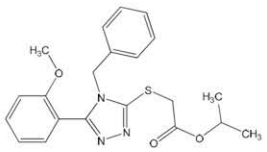

isopropyl 2-(4-benzyl-5-(2-methoxyphenyl)-4*H*-1,2,4-triazol-3-ylthio)acetate

2

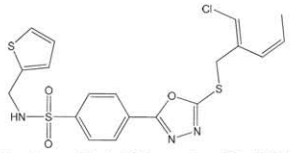

4-(5-(2-chlorobenzylthio)-1,3,4-oxadiazol-2-yl)-*N*-(thiophen-2-ylmethyl)benzenesulfonamide

3

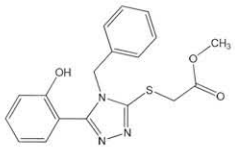

methyl 2-(4-benzyl-5-(2-hydroxyphenyl)-4*H*-1,2,4-triazol-3-ylthio)acetate

4

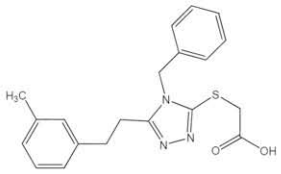

2-(4-benzyl-5-(3-methylphenethyl)-4*H*-1,2,4-triazol-3-ylthio)acetic acid

5

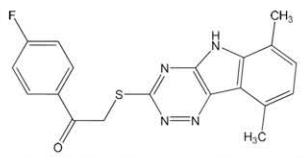

2-(6,9-dimethyl-5*H*-[1,2,4]triazino[5,6-*b*]indol-3-ylthio)-1-(4-fluorophenyl)ethanone

6

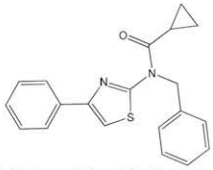

N-benzyl-*N*-(4-phenylthiazol-2-yl)cyclopropanecarboxamide

7

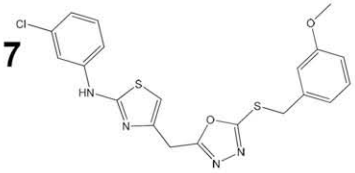

N-(3-chlorophenyl)-4-((5-(3-methoxybenzylthio)-1,3,4-oxadiazol-2-yl)methyl)thiazol-2-amine

8

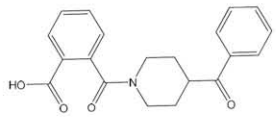

2-(4-benzoylpiperidine-1-carbonyl)benzoic acid

9

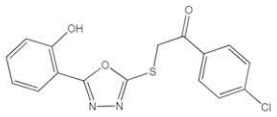

1-(4-chlorophenyl)-2-(5-(2-hydroxyphenyl)-1,3,4-oxadiazol-2-ylthio)ethanone

10

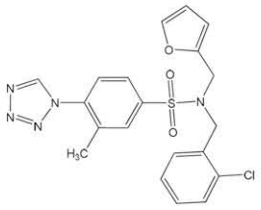

N-(2-chlorobenzyl)-*N*-(furan-2-ylmethyl)-3-methyl-4-(1*H*-tetrazol-1-yl)benzenesulfonamide

11

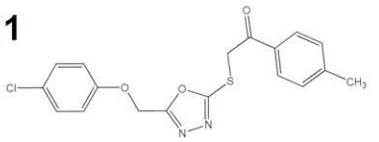

2-(5-((4-chlorophenoxy)methyl)-1,3,4-oxadiazol-2-ylthio)-1-*p*-tolylethanone

12

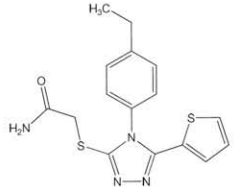

2-(4-(4-ethylphenyl)-5-(thiophen-2-yl)-4*H*-1,2,4-triazol-3-ylthio)acetamide

13

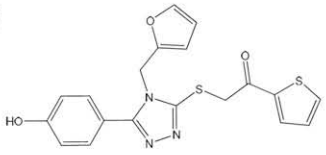

2-(4-(furan-2-ylmethyl)-5-(4-hydroxyphenyl)-4*H*-1,2,4-triazol-3-ylthio)-1-(thiophen-2-yl)ethanone

14

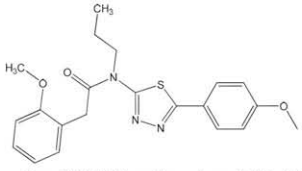

2-(2-methoxyphenyl)-*N*-(5-(4-methoxyphenyl)-1,3,4-thiadiazol-2-yl)-*N*-propylacetamide

15

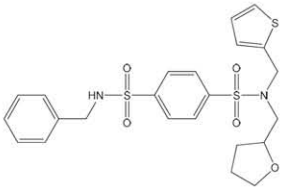

N^1-benzyl-N^4-((tetrahydrofuran-2-yl)methyl)-N^4-(thiophen-2-ylmethyl)benzene-1,4-disulfonamide

16

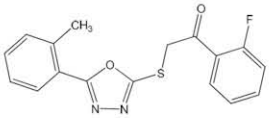

1-(2-fluorophenyl)-2-(5-*o*-tolyl-1,3,4-oxadiazol-2-ylthio)ethanone

17

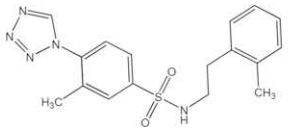

3-methyl-*N*-(2-methylphenethyl)-4-(1*H*-tetrazol-1-yl)benzenesulfonamide

18

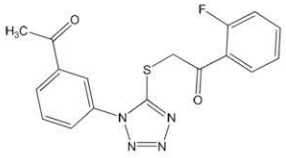

2-(1-(3-acetylphenyl)-1*H*-tetrazol-5-ylthio)-1-(2-fluorophenyl)ethanone

19

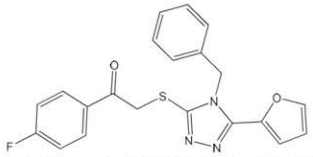

2-(4-benzyl-5-(furan-2-yl)-4*H*-1,2,4-triazol-3-ylthio)-1-(4-fluorophenyl)ethanone

20

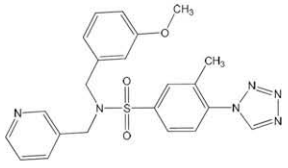

N-(3-methoxybenzyl)-3-methyl-*N*-(pyridin-3-ylmethyl)-4-(1*H*-tetrazol-1-yl)benzenesulfonamide

21

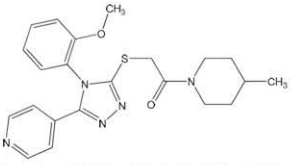

2-(4-(2-methoxyphenyl)-5-(pyridin-4-yl)-4*H*-1,2,4-triazol-3-ylthio)-1-(4-methylpiperidin-1-yl)ethanone

22

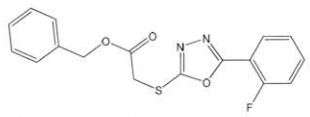

benzyl 2-(5-(2-fluorophenyl)-1,3,4-oxadiazol-2-ylthio)acetate

23

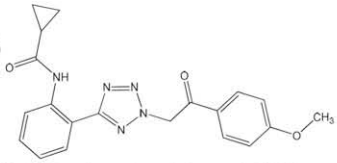

N-(2-(2-(2-(4-methoxyphenyl)-2-oxoethyl)-2*H*-tetrazol-5-yl)phenyl)cyclopropanecarboxamide

24

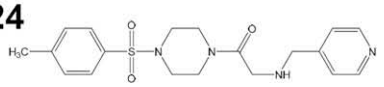

2-(pyridin-4-ylmethylamino)-1-(4-tosylpiperazin-1-yl)ethanone

25

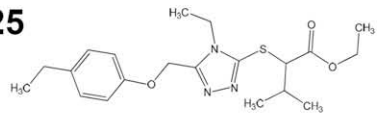

ethyl 2-(4-ethyl-5-((4-ethylphenoxy)methyl)-4*H*-1,2,4-triazol-3-ylthio)-3-methylbutanoate

Fig. 1. Chemical structures of the tested compounds.

consideration a number of factors such as the number of functionalities of the molecules, their bulkiness, stereochemistry and susceptibility to protease attack, as outlined under Experimental protocols. The molecular weight of the selected compounds falls in the range 328–506 Da, with an average value of 388 Da. They contain between 4 and 11 flexible bonds, with the number of hydrogen bond donors and acceptors ranging from 0 to 1 and from 3 to 9, respectively. With only two exceptions (**4** and **8**), no compounds display ionisable groups. The log *P* values range from 0.34 (compound **23**) to 4.60 (compound **16**). Two compounds (**15** and **25**) possess a stereocentre. By comparison, a known inhibitor, BX 528 (MW = 496.3; log *P* = 1.51), possesses 4 and 8 hydrogen bond donors and acceptors, 13 flexible bonds, a carboxylate, and two chiral atoms. Interestingly, this indicates that the retrieved molecules are structurally dissimilar, and have a lower molecular weight than a recognized CP inhibitor.

The presence of five-membered hetero-ring systems is remarkable since 20 out of 25 (representing 80% of the total) contain an oxadiazole, tetrazole, thiadiazole or triazole ring system in their structure. Such ring systems are not uncommon in the literature. 1,3,4-oxadiazoles have been used as amide bond surrogates in benzodiazepine receptor agonists [20], muscarinic receptor agonists [21], neurokinin 1 receptor antagonists [22], antiinflammatory agents [23], and Phe-Gly peptidomimetics [24]. Several non-peptide angiotensin II receptor antagonists like (1-((2′-(2*H*-tetrazol-5-yl)biphenyl-4-yl)methyl)-2-butyl-4-chloro-1*H*-imidazol-5-yl)methanol (Losartan, known by the trade name Cozaar) bear a tetrazole ring [25] while 1,3,4-thiadiazole compounds showed potent matrix metalloproteinase inhibition [26]. Posaconazole, a broad-spectrum orally active antifungal [27], and the hypnotic/sedative benzodiazepine triazolam (marketed under brand names Halcion/Novodorm/Songar) [28], are examples of therapeutic agents containing a triazolyl nucleus. This fact might be related to the high percent of drug-like structures within the screening collection database. Further, it suggests that the high-throughput screening of large databases may provide valuable known fragments that can be assayed against unspotted biological targets.

2.2. Inhibition of metallocarboxypeptidases

The inhibitory ability of the selected test set was evaluated in vitro against two B-type metallocarboxypeptidases, namely corn earworm (*Helicoverpa zea*) CPB (HzCPB), an inhibitor-resistant digestive protease from a lepidopteran pest insect [29], and human CPB (hCPB), a disease-linked metallocarboxypeptidase. Bovine CPA (bCPA1), a model zinc-dependent protease, was included in the assay given the structural proximity among M14 A- and B-type proteins. As can be seen in Table 1, the inhibitory potency falls in the lower micromolar range, with five compounds (20% of the total) showing K_i values below 10 μM. Inhibition of bCPA1 was also detected, but it was weaker as compared to that of CPB in most cases. The values for the best compounds are comparable to those for two well-known reference inhibitors [30,31] also included in Table 1.

Interestingly, the three most potent CPB inhibitors, **3**, **6** and **7**, harbor three different chemical classes of five-membered hetero-rings: 1,2,4-triazole, thiazole, and 1,3,4-oxadiazole, respectively. Compound **3**, methyl 2-(4-benzyl-5-(2-hydroxyphenyl)-4*H*-1,2,4-triazol-3-ylthio)acetate, shows a 30-fold CPB/CPA inhibitory ratio, suggesting some specific mode of action. This ratio increases to 160-fold in the case of **6**, *N*-benzyl-*N*-(4-phenylthiazol-2-yl)cyclopropanecarboxamide, while **7**, *N*-(3-chlorophenyl)-4-((5-(3-methoxybenzylthio)-1,3,4-oxadiazol-2-yl)methyl)thiazol-2-amine, exerted the most potent human CPB inhibitory effect, its K_i being 1.2 μM, although with a moderate 20-fold CPB/CPA ratio. The latter is an extended molecule (four planar rings) whereas compounds, **3** and **6** display three planar systems, suggesting that **7**, which is also the best among 1,3,4-oxadiazoles (namely, **2**, **9**, **11**, **16**, **22**), is ideally suited to bind the CPB active site cleft. Compound **2** is comparable in size to **7**, but it behaves as a poor human CPB inhibitor (K_i = 40.0 μM), probably indicating a less well tailored structure.

Compounds retrieved from the high-throughput virtual screening survey are listed in descending docking energy value in Table 1. It is clear that docking energy ranking scores do not strictly correlate with the measured K_i values. For example, for the 25% top ranked in docking energy (compounds **1**–**7**), only four (57%) are within the 25% best K_i values, and only one of them, **3**, matches the ranking in both categories, while **7**, which ranks first in K_i value and is the most potent human CPB inhibitor, is only 7th in docking energy. Three of the top 25% best scores in docking energy (compounds **2**, **4**, and **5**) fall well below the tenth position in the K_i value ranking. Compounds **2** and **7**, belonging to the same 1,3,4-oxadiazole class showed opposite behaviours as, although **2** is a poor human CPB inhibitor, it scores better than **7**. An inspection of their structures revealed that the 1,3,4-oxadiazole ring is directly joined to the bulky benzenesulfonamide moiety in **2**, while the substituent group in **7** is bonded through a methylene spacer. This could reduce the flexibility of **2** and impair the placing of its 1,3,4-oxadiazole in the zinc coordination sphere. Otherwise, we might conceive that the contribution of the sulfonamide group to binding was overestimated or even misplaced during the screening process.

Compounds **1**, **3**, and **4** are 1,2,4-triazoles. While **1** and **3** show a good agreement between docking energy score and K_i value, **4** deviates from this trend, and is indeed one of the poorest inhibitors. The structures of these compounds are similar, but **4** displays a free carboxylate while the other compounds are the methyl and isopropyl esters. A possible explanation for these data is that the free carboxylate might have been overestimated as a binding group by the docking algorithm. Overall, the fact that the predictions were poor for some compounds might be ascribed to some weaknesses of the docking algorithm to handle certain types of chemical bonding (i.e., the coordination sphere of the zinc ion and its ligands) or to our manual knowledge-based filtering procedure, which was based on structural inspection rather than on docking energy scores.

Although others had reported on five-membered hetero-rings like imidazole as CPA and CPB inhibitors [32–36], none of them has yet reached the clinical practice for the treatment of diseases related to the M14 family of proteases. Thus, the 1,3,4-oxadiazole containing compounds can be regarded as a new type of small-molecule inhibitors of various proteases belonging to the M14 family. To better understand the behaviour of this new type of compounds we performed molecular docking of selected 1,3,4-oxadiazole inhibitors to different M14 target proteins.

2.3. Analysis of 1,3,4-oxadiazole binding to metallocarboxypeptidases

Compound **7** was chosen for molecular docking based on its behaviour as the most potent inhibitor of the tested set. The docking procedure was validated by redocking of known crystal complex structures. Although the overall quality of the redocking was satisfactory in terms of rmsd values (see Experimental protocols for details), a failure to predict a salt bridge in one of the cases implies that the reliability of the atomic distances derived from the docking procedures is not absolute.

Since compound **7** inhibits both the human and insect CPB counterparts with fairly similar potency, docking was initially carried out in parallel. As expected, the binding to insect CPB proceeds much like that to the human counterpart, so we focused

Table 1
Inhibitory constants[a] and docking energy values.[b]

Compound	bCPA1[c]	hCPB	HzCPB	Docking energy	Compound	bCPA1[c]	hCPB	HzCPB	Docking energy
1	160.0	7.4	36.1	−12.63	**15**	19.4	23.0	–	−11.03
2	67.3	40.0	1.4	−12.06	**16**	39.3	14.7	40.0	−11.01
3	159.0	4.9	41.6	−11.75	**17**	138.0	25.9	38.0	−10.82
4	217.0	196.0	57.0	−11.67	**18**	550.0	33.6	53.8	−10.82
5	86.3	15.0	9.0	−11.64	**19**	236.0	74.5	–	−10.65
6	800.0	4.5	1.2	−11.53	**20**	148.0	23.9	28.4	−10.58
7	22.5	1.2	3.6	−11.27	**21**	381.0	20.8	30.2	−10.47
8	320.0	20.7	19.6	−11.25	**22**	32.0	67.2	33.4	−10.46
9	2.1	7.5	1.0	−11.23	**23**	41.3	292.0	31.0	−10.44
10	159.0	16.6	12.6	−11.22	**24**	250	364.0	18.0	−10.42
11	36.7	11.7	12.0	−11.13	**25**	22.0	10.8	11.9	−10.05
12	155.0	11.6	27.2	−11.11	**BzlSA**[d]	0.5	10.0	11.9	
13	74.5	9.1	–	−11.08	**GEMSA**[e]	nd	1.1	nd	
14	128.0	25.1	19.7	−11.07					

[a] Measured K_i value (μM); (–), no inhibition observed at the highest concentration tested; nd: no data available.
[b] Compounds are ordered in descending docking energy value, in kcal/mol.
[c] bCPA1, bovine carboxypeptidase A1; hCPB, human carboxypeptidase B; HzCPB, carboxypeptidase B from corn earworm (*Helicoverpa zea*).
[d] BzlSA, DL-benzylsuccinic acid.
[e] GEMSA, DL-guanidinoethylmercaptosuccinic acid.

our analysis on the vertebrate enzyme, comparing the putative CPB/**7** complex structure with a known CPB/peptide inhibitor structure. Besides, to better characterize the fairly selective CPB binding mode, we also analyzed the **7**-docked CPA structure. From that comparison, striking differences in the binding of **7** to CPA and CPB arised that deserved further analysis, as will be discussed below.

The predicted binding of **7** to human CPB suggests that it involves the zinc ion and key residues lining the active site cleft (Fig. 2). One of the nitrogen atoms of the 1,3,4-oxadiazole ring coordinates the zinc ion (at 2.3 Å), while the other forms a strong hydrogen bond to the carbonyl O atom of Ser197 (a residue at subsite S2). The oxadiazolyl O atom forms hydrogen bonds (at 2.9 Å) to the Tyr248 phenolic hydroxyl and to the Glu270 Oε2 atom (3.1 Å). In this way, the 1,3,4-oxadiazole hetero-ring is engaged in interactions with key catalytic residues at the S1′ and S1 subsites. The 1,3,4-oxadiazole hetero-ring seems to bissect the molecule in two parts: the methoxyphenyl moiety becomes buried into the CPB specificity pocket while the chlorobenzyl group is left just at the entrance of the active site cleft. In the former, the methoxy oxygen atom forms a strong hydrogen bond to Ser207 hydroxyl (at 2.7 Å), while the aromatic ring is placed in a wide hydrophobic environment sustained by Ile203, Gly243, Ile247, Ala250, and Thr268. The methoxy oxygen atom appears too far (at a distance >3.5 Å) and probably is not hydrogen bonded to Asp255, the specificity determinant residue in CPB. Some other atoms of the chlorobenzyl and the adjacent thiazole ring seem to be less favourably engaged in interactions to residues lining the active site cleft. The sulfur atom of the thiazole ring linking the chlorobenzyl and the 1,3,4-oxadiazole hetero-ring contributes marginally to binding (no interaction of this atom with any protein residue was observed). The sulfur atom is at 3.2 Å from Tyr198 phenolic hydroxyl and at almost 3.9 Å from a carbon atom of Phe279 aromatic ring (Tyr198 and Phe279 are in the S2 and S3 subsites, respectively).

A clear difference was evident from the comparison of the complexes of CPA and CPB with compound **7** (Fig. 3). In bCPA1, the methoxyphenyl aromatic ring is placed in an environment similar to that in CPB. However, the bulky Ile243 side chain in bCPA1

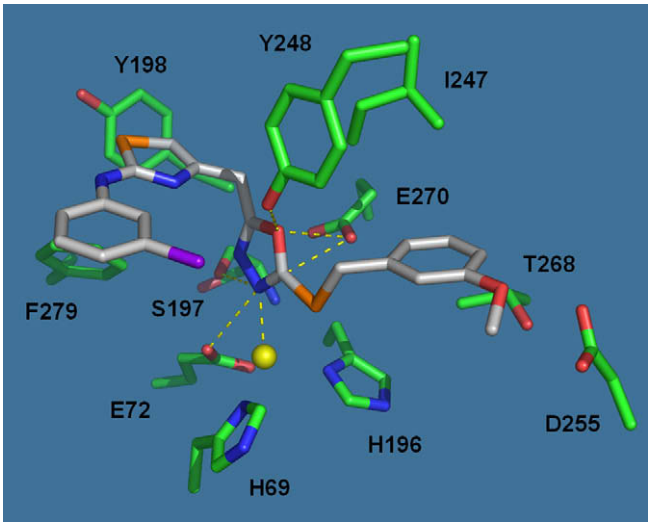

Fig. 2. A view of the putative binding of inhibitor **7** (stick model, white carbons) in the active site of human CPB. The 1,3,4-oxadiazole ring engages two catalytically important residues, Tyr248 and Glu270 as well as the Zn^{2+} ion. CPB side chains at a distance <5 Å from compound **7** are depicted in stick model. The Zn^{2+} ion is shown as a yellow sphere. Other residues important for binding are labelled. Carbon: green, sulfur: orange, nitrogen: blue, oxygen: red and chlorine: magenta.

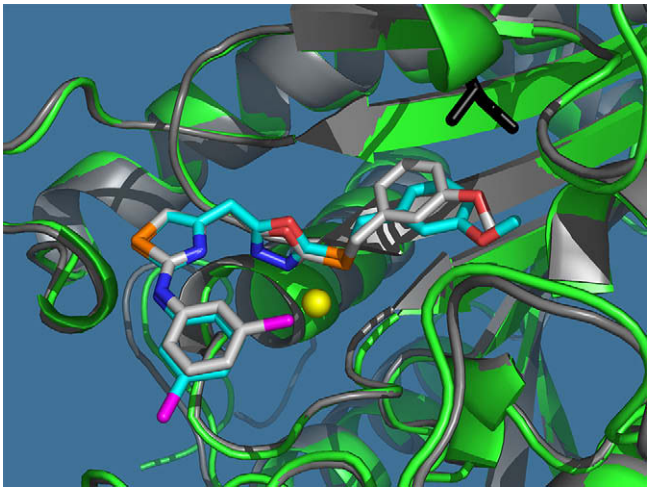

Fig. 3. Superimposition of the complexes of inhibitor **7** with CPA and CPB. Compound **7** (white carbons in CPB, light blue in CPA) is shown in stick model. CPB (green) and CPA (grey) are in cartoon representation. The Zn^{2+} ion is shown as a yellow sphere. Ile243 in CPA is highlighted black (a glycine is in the equivalent position in CPB) to mark the offset of **7**. Approximately the same orientation as in Fig. 2.

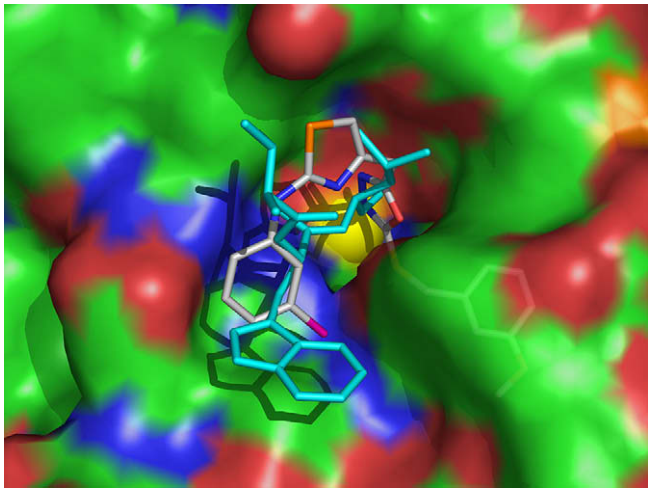

Fig. 4. CPB in complex with inhibitor **7** (white carbons) compared to the complex with tick proteinaceous inhibitor, TCI. Only the three C-terminal residues from TCI, Val72–Trp73–Leu74 (cyan carbons), are shown. The Zn^{2+} ion is coloured yellow and CPB as a translucent surface in atom-type colour. The bulge located south-east from the Zn ion corresponds to the catalytically crucial Tyr248. The view corresponds approximately to the orientation displayed in Fig. 2 after a 70° rotation downwards.

(the equivalent CPB residue is Gly243) is in close proximity to the phenyl ring of the methoxyphenyl moiety, leading to a steric clash between them. As a result, this group is displaced, probably resulting in an impaired binding of the inhibitor to bCPA1 and causing a drop in inhibitory potency. This emphasizes that an aromatic fragment placed at this position in the 1,3,4-oxadiazole scaffold might be of help in the design of CPB specific variants.

As compared to the structure of CPB bound to the proteinaceous inhibitor from ticks, TCI, the binding of the chlorobenzyl moiety recalls that of the penultimate tryptophan residue from the peptidic inhibitor (Fig. 4). From this comparison another point of optimization of the 1,3,4-oxadiazole scaffold arises, as the chlorobenzyl group makes a suboptimal interaction that demands a larger aromatic moiety. The outcome from the molecular docking experiment illustrates that the 1,3,4-oxadiazole scaffold is ideally adapted to attach to key residues at the active site of B-type carboxypeptidases, while there are points beyond this scaffold that perform a less advantageous exploitation of anchorage points and may therefore be taken into consideration as a subject for further improvement.

3. Conclusion

Following a high-throughput virtual screening survey, we obtained new five-membered hetero-ring inhibitors of metallocarboxypeptidases. The poses retrieved from the screening display chemical fragments found in several marketed drugs, indicating the drug-like content of the screening database. Once obtained, these known chemical fragments were then challenged against untried biological targets. Some of the selected poses performed an inhibitory activity against the target protein. The screening procedure performed efficiently regarding the top ranked compounds, as the docking energy scores reflect the measured K_i values. For other compounds the predictions were poor, either due to some weaknesses of the docking algorithm or to our particular knowledge-based filtering methodology.

The most active compounds show different five-membered hetero-ring structures, and exert potent human CPB inhibition. In particular, **7**, *N*-(3-chlorophenyl)-4-((5-(3-methoxybenzylthio)-1,3,4-oxadiazol-2-yl)methyl)thiazol-2-amine, is a low micromolar inhibitor of this enzyme. This compound features an unprecedented 1,3,4-oxadiazole five-membered hetero-ring scaffold, distinct from known M14 small-molecule inhibitors. From molecular docking simulations of **7** and comparison to a known peptide inhibitor, some points of improvement can be suggested that might lead to an optimized version. We envisage that these modifications could yield second generation compounds with improved features in terms of inhibition profiles and selectivity. Therefore, the 1,3,4-oxadiazole scaffold is proposed as an interesting lead for further development.

4. Experimental protocols

4.1. General procedures and materials for the biological experiments

Human CPB, and corn earworm (*H. zea*) CPB, were recombinantly expressed as the zymogen form in the methylotrophic *Pichia pastoris* system. They were then proteolytically converted to the mature, enzymatically active, form as published [29,37]. Bovine pancreatic CPA was from Sigma. Enzyme concentrations for the kinetic studies were kept fixed at typically 5–50 nM. Two chromogenic synthetic substrates (Bachem, Bubendorf, Switzerland) were used: *N*-(4-methoxyphenylazoformyl)-Phe-OH (Aaf-Phe-OH; K_m for CPA: 100 μM) and *N*-(4-methoxyphenylazoformyl)-Arg-OH (Aaf-Arg-OH; K_m for CPB: 60 μM). The assay concentrations for Aaf-Phe-OH and Aaf-Arg-OH were 100 and 60 or 200 μM, respectively. The experimental assays were performed at room temperature in 50 mM Tris, 0.5 M NaCl, pH 7.5 buffer for CPA and in 20 mM Tris, 0.1 M NaCl, pH 7.5 buffer for CPB, with variable concentrations of the analyzed compounds between 50 nM and 250 μM. The initial velocity measurements were performed at least per triplicate at room temperature in a Victor3 microtiter plate reader (PerkinElmer, Waltham, MA, USA), following the changes in absorbance continuously at 340 nm. Data were fed into the GraphPad Version 5.0 package (GraphPad Software, San Diego, CA, USA) that was used to derive the kinetic parameters. The inhibition was fitted to a competitive, one-site model, with a good agreement to the experimental observations. The K_i value was then calculated from the IC_{50} following the procedure by Cheng and Prussoff [38].

4.2. Bioinformatics: screening procedures

The ArgusDock molecular modelling engine [39] implemented within the package ArgusLab Version 4.0.1 (www.arguslab.com) was used to query the ASINEX Platinum (APC) screening collection (version of August 2006; size > 125,000). The APC is a diverse, non-focused, non-prefiltered, small-molecule screening collection and contains a high percentage of drug-like molecules [40]. The screening procedure was run on bench top PCs under Windows. To ease the screening procedure, the APC was divided into small size sub-libraries (2500 compounds each) with CORINA [41]. The final set of poses was obtained after coarse minimization, re-clustering and ranking. The 10 lowest-energy poses were retained from each sub-library, and were stored for further analysis.

The 500 lowest-energy poses were then analyzed with the FAFDrugs server (http://bioserv.rpbs.jussieu.fr/FAFDrugs.html) [42]. The properties monitored included molecular weight, number of hydrogen bond acceptors and donors, number of flexible and rigid bonds, number of carbon and hetero-atoms, estimation of the partition coefficient (log *P*), and calculation of polar surface area. This automatic procedure was followed by a careful, knowledge-based, manual filtering to yield a selected final set. The knowledge-based manual filtering was performed by visual inspection of the compounds, which were selected from the preference of CPs to

bind to short peptides, applying the following general rules: i) compounds containing a linear and extended backbone having 3–5 functionalities (i.e. ring systems and/or trigonal planar sp^2-carbons, joined by single bonds) were preferred as the first choice; ii) compounds having bulky systems, like those containing three or more fused rings, and tribenzene-containing molecules, were discarded; iii) compounds having stereogenic centres were also disregarded; and iv) structures containing a chemical linkage susceptible to be hydrolyzed by the target enzyme were also eliminated.

The 3D crystal structure of human CPB (coordinates file code: 1zli) was used for the screening. After removal of ligands, a box centred at the catalytic zinc was defined as the binding site. The size of the box, $20 \times 15 \times 20$ Å, encompasses all the known subsites for substrate binding, thus allowing a complete sampling of the CPB active site cleft. A flexible ligand docking was employed.

4.3. Bioinformatics: molecular docking

The structural analysis of the most potent inhibitors was carried out by molecular docking with the AutoDock 4 package [43]. A binding box was built, centred at the catalytic zinc ion with a size defined to encompass all known binding sites in the active site. The lowest-energy conformer was used for the discussion and a careful analysis of hydrogen bonds and intermolecular interactions was performed. The approach was validated by redocking of small-molecules appearing in known crystal complex structures: L-phenyllactate for CPA (PDB code 2ctc) and an imidazole inhibitor for CPB (PDB code 2jew). Redocking was correct in terms of global conformation, orientation of the ligand and rmsd values (0.22 Å and 0.62 Å for L-phenyllactate and the imidazole, respectively). In the latter case, the docking correctly predicted the coordination of the zinc and the hydrogen bond between the terminal NH_2 and Asp255. However, it failed to predict a salt bridge between the ligand and Arg145. A superimposition of compound **7** and the known imidazole inhibitor showed a similar orientation and location of the five-membered rings. The human CPB structure in complex to a proteinaceous inhibitor from ticks (PDB code 1zli) was used for comparison and superimposition. Programs of the Collaborative Computational Project Number 4 suite [44] were used to analyze protein–ligand interactions. Visualization and molecular graphics were done with ArgusLab 4.0.1 (www.arguslab.com) or with PyMol (www.pymol.org). All the final figures were prepared with PyMol.

Acknowledgements

Support by grants BIO2007-68046 (Ministerio de Educación y Ciencia, Spain), 2005SGR-1037 (Generalitat de Catalunya) and CAMP project 108830 (VI EU Framework Programme) is gratefully acknowledged. DF wishes to thank the European Union Alβan Programme for a PhD fellowship (contract no. E04D035150AR).

References

[1] J. Vendrell, F.X. Aviles, L.D. Fricker, Metallocarboxypeptidases, in: A. Messerschmidt, W. Bode, M. Cygler (Eds.), Handbook of Metalloproteins, John Wiley and Sons Ltd., Chichester, 2004, pp. 176–189.
[2] M. Rodriguez de la Vega, R.G. Sevilla, A. Hermoso, J. Lorenzo, S. Tanco, A. Diez, L.D. Fricker, J.M. Bautista, F.X. Aviles, FASEB J. 21 (2007) 851–865.
[3] H. Wang, Q. Zhou, J.W. Kesinger, C. Norris, C. Valdez, Exp. Biol. Med. (Maywood) 232 (2007) 1170–1180.
[4] Q. Zhou, A.C. Law, J. Rajagopal, W.J. Anderson, P.A. Gray, D.A. Melton, Dev. Cell 13 (2007) 103–114.
[5] C.A. Muller, S. Appelros, W. Uhl, M.W. Buchler, A. Borgstrom, Gut 51 (2002) 229–235.
[6] S. Asai, T. Sato, T. Tada, T. Miyamoto, N. Kimbara, N. Motoyama, H. Okada, N. Okada, J. Immunol. 173 (2004) 4669–4674.
[7] J.L. Willemse, D.F. Hendriks, Front. Biosci. 12 (2007) 1973–1987.
[8] F. Fialka, R.M. Gruber, R. Hitt, L. Opitz, E. Brunner, H. Schliephake, F.J. Kramer, Oral Oncol. 44 (2008) 941–948.
[9] O. Hataji, O. Taguchi, E.C. Gabazza, H. Yuda, C.N. D'Alessandro-Gabazza, H. Fujimoto, Y. Nishii, T. Hayashi, K. Suzuki, Y. Adachi, Am. J. Hematol. 76 (2004) 214–219.
[10] P. Cronet, W. Knecht, C.A.-C. Malmborg Hager, M. Andersson, C. Furebring, Sequences of modified human carboxypeptidase U (CPU) with increased thermal stability for treating hemorrhage disorders, Astrazeneca AB, Swed., Astrazeneca UK Limited, Application: WO. Patent No. 2005052149, 2005.
[11] S. Golz, U. Brueggemeier, A. Geerts, Diagnostics and therapeutics for diseases associated with human carboxypeptidase A3 based on tissue expression profiling, Bayer Healthcare AG, Germany, Application: WO. Patent No. 2006010495, 2006.
[12] S. Golz, U. Brueggemeier, A. Geerts, Diagnostics and therapeutics for diseases associated with human carboxypeptidase A2 based on tissue expression profiling, Bayer Healthcare AG, Germany, Application: WO. Patent No. 2006010499, 2006.
[13] S. Matsugi, T. Hamada, N. Shioi, T. Tanaka, T. Kumada, S. Satomura, Clin. Chim. Acta 378 (2007) 147–153.
[14] O. Yanes, J. Villanueva, E. Querol, F.X. Aviles, Nat. Protoc. 2 (2007) 119–130.
[15] M.S. Buchanan, A.R. Carroll, A. Edser, M. Sykes, G.A. Fechner, P.I. Forster, G.P. Guymer, R.J. Quinn, Bioorg. Med. Chem. Lett. 18 (2008) 1495–1497.
[16] S.H. Wang, S.F. Wang, W. Xuan, Z.H. Zeng, J.Y. Jin, J. Ma, G.R. Tian, Bioorg. Med. Chem. 16 (2008) 3596–3601.
[17] Y.X. Wang, V. da Cunha, J. Vincelette, L. Zhao, M. Nagashima, K. Kawai, S. Yuan, K. Emayan, I. Islam, J. Hosoya, M.E. Sullivan, W.P. Dole, J. Morser, B.O. Buckman, R. Vergona, Thromb. Haemostasis 97 (2007) 54–61.
[18] Y.X. Wang, L. Zhao, M. Nagashima, J. Vincelette, D. Sukovich, W. Li, B. Subramanyam, S. Yuan, K. Emayan, I. Islam, P. Hrvatin, J. Bryant, D.R. Light, R. Vergona, J. Morser, B.O. Buckman, Thromb. Haemostasis 97 (2007) 45–53.
[19] D. Fernandez, O. Illa, F.X. Aviles, V. Branchadell, J. Vendrell, R.M. Ortuno, Bioorg. Med. Chem. 16 (2008) 4823–4828.
[20] W.R. Tully, C.R. Gardner, R.J. Gillespie, R. Westwood, J. Med. Chem. 34 (1991) 2060–2067.
[21] B.S. Orlek, F.E. Blaney, F. Brown, M.S. Clark, M.S. Hadley, J. Hatcher, G.J. Riley, H.E. Rosenberg, H.J. Wadsworth, P. Wyman, J. Med. Chem. 34 (1991) 2726–2735.
[22] T. Ladduwahetty, R. Baker, M.A. Cascieri, M.S. Chambers, K. Haworth, L.E. Keown, D.E. MacIntyre, J.M. Metzger, S. Owen, W. Rycroft, S. Sadowski, E.M. Seward, S.L. Shepheard, C.J. Swain, F.D. Tattersall, A.P. Watt, D.W. Williamson, R.J. Hargreaves, J. Med. Chem. 39 (1996) 2907–2914.
[23] M.D. Mullican, M.W. Wilson, D.T. Connor, C.R. Kostlan, D.J. Schrier, R.D. Dyer, J. Med. Chem. 36 (1993) 1090–1099.
[24] S. Borg, R.C. Vollinga, M. Labarre, K. Payza, L. Terenius, K. Luthman, J. Med. Chem. 42 (1999) 4331–4342.
[25] D.H. Smith, Drugs 68 (2008) 1207–1225.
[26] J.Y. Winum, A. Scozzafava, J.L. Montero, C.T. Supuran, Med. Res. Rev. 26 (2006) 767–792.
[27] J.E. Frampton, L.J. Scott, Drugs 68 (2008) 993–1016.
[28] G.E. Pakes, R.N. Brogden, R.C. Heel, T.M. Speight, G.S. Avery, Drugs 22 (1981) 81–110.
[29] A. Bayes, M. Comellas-Bigler, M. Rodriguez de la Vega, K. Maskos, W. Bode, F.X. Aviles, M.A. Jongsma, J. Beekwilder, J. Vendrell, Proc. Natl. Acad. Sci. U.S.A. 102 (2005) 16602–16607.
[30] L.D. Byers, R. Wolfenden, Biochemistry 12 (1973) 2070–2078.
[31] T.J. McKay, A.W. Phelan, T.H. Plummer Jr., Arch. Biochem. Biophys. 197 (1979) 487–492.
[32] J.C. Barrow, P.G. Nantermet, S.R. Stauffer, P.L. Ngo, M.A. Steinbeiser, S.S. Mao, S.S. Carroll, C. Bailey, D. Colussi, M. Bosserman, C. Burlein, J.J. Cook, G. Sitko, P.R. Tiller, C.M. Miller-Stein, M. Rose, D.R. McMasters, J.P. Vacca, H.G. Selnick, J. Med. Chem. 46 (2003) 5294–5297.
[33] M.E. Bunnage, J. Blagg, J. Steele, D.R. Owen, C. Allerton, A.B. McElroy, D. Miller, T. Ringer, K. Butcher, K. Beaumont, K. Evans, A.J. Gray, S.J. Holland, N. Feeder, R.S. Moore, D.G. Brown, J. Med. Chem. 50 (2007) 6095–6103.
[34] M.S. Han, D.H. Kim, Bioorg. Med. Chem. Lett. 11 (2001) 1425–1427.
[35] K.J. Lee, K.C. Joo, E.J. Kim, M. Lee, D.H. Kim, Bioorg. Med. Chem. 5 (1997) 1989–1998.
[36] P.G. Nantermet, J.C. Barrow, S.R. Lindsley, M. Young, S.S. Mao, S. Carroll, C. Bailey, M. Bosserman, D. Colussi, D.R. McMasters, J.P. Vacca, H.G. Selnick, Bioorg. Med. Chem. Lett. 14 (2004) 2141–2145.
[37] S. Ventura, V. Villegas, J. Sterner, J. Larson, J. Vendrell, C.L. Hershberger, F.X. Aviles, J. Biol. Chem. 274 (1999) 19925–19933.
[38] Y. Cheng, W.H. Prusoff, Biochem. Pharmacol. 22 (1973) 3099–3108.
[39] S. Joy, P.S. Nair, R. Hariharan, M.R. Pillai, In Silico Biol. 6 (2006) 601–605.
[40] M. Krier, G. Bret, D. Rognan, J. Chem. Inf. Model. 46 (2006) 512–524.
[41] J. Gasteiger, C. Rudolph, J. Sadowski, Tetrahedron Comput. Methodol. 3 (1990) 537–547.
[42] M.A. Miteva, S. Violas, M. Montes, D. Gomez, P. Tuffery, B.O. Villoutreix, Nucleic Acids Res. 34 (2006) W738–W744.
[43] G.M. Morris, D.S. Goodsell, R.S. Halliday, R. Huey, W.E. Hart, R.K. Belew, A.J. Olson, J. Comput. Chem. 19 (1998) 1639–1662.
[44] Collaborative Computational Project, Acta Crystallogr., Sect. D: Biol. Crystallogr. 50 (1994) 760–776.